

Article

Simplified Model for Strengthening Design of Beam–Column Internal Joints in Reinforced Concrete Frames

Antonio Bossio ¹, Francesco Fabbrocino ², Gian Piero Lignola ^{1,*}, Andrea Prota ¹
and Gaetano Manfredi ¹

¹ Department of Structures for Engineering and Architecture, University of Naples Federico II, Via Claudio, 21, 80125 Napoli, Italy; E-Mails: antonio.bossio@unina.it (A.B.); aprota@unina.it (A.P.); gamanfre@unina.it (G.M.)

² Department of Engineering, Telematic University Pegaso, Piazza Trieste e Trento, 48, 80132 Napoli, Italy; E-Mail: francesco.fabbrocino@unipegaso.it

* Author to whom correspondence should be addressed; E-Mail: glignola@unina.it; Tel.: +39-081-768-3492; Fax: +39-081-768-5921.

Academic Editors: Alper Ilki and Masoud Motavalli

Received: 1 August 2015 / Accepted: 31 August 2015 / Published: 10 September 2015

Abstract: The beam-column joints are very restricted areas in which the internal forces, generated by boundary elements, act on the concrete core and reinforcing bars with a very high gradient. They are the link between horizontal and vertical structural elements, and therefore, they are directly involved in the transfer of seismic forces. Thus, they are crucial to study the seismic behavior of reinforced concrete (RC) structures. To fully understand the seismic performances and failure modes of beam-column joints in RC buildings, a simplified analytical model of joint behavior is proposed and theoretical simulations are performed. The aim of the model, focusing on internal perimeteric joints, is to identify the strength hierarchy in terms of capacity for different failure modes (namely failure of cracked joint, bond failure of passing through bars, flexural/shear failures of columns or beams). It could represent a tool for the designers of new joints to quantify the performance of new structures, but also as a tool for the designers of external strengthening of existing joints in order to calculate the benefits of the retrofit and pushing the initial failure to a more desirable failure mode. Further, some experimental results of tests available in the scientific literature are reported, analyzed and compared.

Keywords: beam-column joints; analytical modeling; capacity; failure mode; FRP; reinforced concrete

1. Introduction

The behavior of the beam-column joint is a crucial aspect in a new or existing reinforced concrete (RC) moment resisting frame and needs to be designed and detailed properly. During earthquakes, the failure of beam-column joints is governed by bond and shear failure mechanisms which are usually brittle. Beam-column joints having deficient reinforcement details are expected to respond poorly, even when subjected to moderate seismic action. Beam-column joints in a RC moment resisting frame are circumscribed portions of the structures where high loads transfer between the connecting elements (*i.e.*, columns and beams) in the structure. This aspect can be particularly crucial in the case of seismically-resistant frames where this high demand mobilizes the inelastic capacity of RC members to dissipate seismic energy while joints are poorly designed, jeopardizing the entire structure, even if it is correctly designed (Manfredi *et al.*) [1].

Under certain seismic actions, the beams connecting into a joint are subjected to moments in the same (clockwise or counter-clockwise) direction. Under these moments, the bars at the same level are pulled or pushed in the same direction at both sides of the joint panel. If the column is not wide enough, or if the strength of concrete in the joint is too low, the bond between steel bars and concrete cannot balance this stress request (Lignola *et al.*) [2]. In such cases, the reinforcement bars slip inside the joint region, and beams lose their load capacity. Furthermore, under cyclic actions, joints undergo the diagonal push and pull actions and concrete diagonally cracks into the joint panel.

Stirrups in the joint panel provide the crucial shear strength and confinement pressure to preserve joint panels from premature brittle failures. A proper quantity of transverse reinforcement allows the stresses to be appropriately transmitted between the beams and columns. Nonetheless, the deficiency of transverse reinforcement in joint panels occurs often in structural systems designed for gravity loads or according to outdated seismic codes (Masi *et al.*) [3]. Hence, current research efforts concentrated on developing cost-effective and sound retrofit techniques and strategies by means of composite materials. Former rehabilitation techniques, such as RC or steel jackets, have been well investigated in the past (e.g., Alcocer and Jirsa [4], Ghobarah *et al.* [5], Tsonos [6], and Hakuto *et al.* [7] among others). In recent years, Fiber-reinforced polymer (FRP) has been widely studied as a novel strengthening system, and it has been extensively applied in practice due to its benefits, such as light weight, high strength, corrosion resistance, and fast constructability.

Several FRP-strengthening materials and layouts were considered to define the benefits provided to the seismic performance of beam-column joints (e.g., Gergely *et al.* [8], Pantelides *et al.* [9], Gergely *et al.* [10], Granata and Parvin [11], Ghobarah and Said [12], Pantelides *et al.* [13] among others).

From a designer point of view, current building codes for an earthquake-resistant design of RC moment frame structures provide an empirical limit on joint shear force. Earlier models, namely, traditional truss and strut models to explain the shear resistance mechanism, were proposed by

Paulay *et al.* [14]. Further studies established shape factors given as empirical factors based on laboratory testing to take into account the variation of beam-column joint configurations. Such studies converged in different seismic code provisions and a review of them for joints, from main codes of practice around the world, can be found in Uma and Jain [15]. However they lack consideration for the effects of other critical factors such as the magnitude of column axial load or the capacity of the members' framing to the joint. Shiohara, in 2001 [16], made some of the first efforts to identify all the crucial factors by means of a mechanical model, as described in the following, being the basis of the improvements provided by the proposed novel model. Re-evaluating available experimental results, the idea was not to limit the joint failure to an exceedance of a joint shear stress capacity (because joint shear stress does not degrade as the storey shear does during experimental tests).

Lowes and Altoontash, in 2003 [17], and in the following years with further improvements and calibrations, proposed a nonlinear model for beam-column joints to be used in numerical analyses to evaluate the impact of joints on RC frame earthquake performance and their deformability, including bond-slip behavior. Increasing the complexity, further studies involved the full nonlinear finite element modeling (FEM) of joints clarifying the role of many factors in the behavior of beam column joints (e.g., Manfredi *et al.* [1] and Lignola *et al.* [2], among others).

2. Research Significance

The aim of the present paper is to investigate the internal RC beam-column joints in order to study seismic behavior and to establish the strength hierarchy in the case of failure. It aims to contribute to capacity design (and the subsequent strength hierarchy) principles. In fact, these modern design principles are strongly subordinate to the beam-column joint panels' behavior which can reduce substantially the global ductility, if the joint is subjected to a premature failure. Theoretical simulations and analytical models have been presented and discussed, and theoretical outcomes have been compared to experimental results. Presented theoretical approach aims to represent a practical tool to be used by practitioners in the FRP-strengthening design process of beam column joints.

3. Basis of Theoretical Model

The study focuses on internal joints which can be identified in a perimetric moment resisting frame. Perimetric frames have been selected because they have less beneficial effect of confinement provided by out-of-plane members (*i.e.*, transverse beams or slabs). Internal joints present two beams framing into the sides of a column.

Experimental joint failure databases (e.g., Kim [18] collected data on 341 subassemblies) highlight typical shear failures in conjunction with, but also without, yielding of longitudinal beam reinforcement. Influencing parameters for joint shear behavior are linked to key points on capacity curves displaying the most distinct stiffness changes. Concrete cracking is usually coupled to yielding or bond failure of longitudinal reinforcement of beams when the most different changes in stiffness, for both overall and local behavior are triggered, up to the point of initiation of joint shear failure (maximum experimental storey shear).

The examined parameters for joint behavior are material properties, joint panel geometry, reinforcement in joint panel, column axial load, and reinforcement bond condition. Furthermore, the

effect of external strengthening, e.g., by means of externally-bonded FRP, but not limited to it, is another debated parameter. Obviously, shear and flexural capacity of intersecting elements, namely beams and columns, are also of interest for the capacity design, hence they are considered herein, but not analyzed in detail, since they are considered almost well established, both in terms of as-built and retrofitted capacity.

The proposed model moves from the so called quadruple flexural resistances model [16] sketched in Figure 1. It considers the kinematics of the four segments divided by diagonal cracks in the joint panel, rotating due to bending moment and shear coming from beams and columns. The equilibrium of internal forces in steel and concrete, and external forces acting on beam ends and column ends is taken into account, whereas the compatibility condition is not necessarily satisfied. Dowel effects of bars and shear friction along diagonal cracks were neglected in the original formulation. In fact, the model, as it was originally proposed, presents some essential assumptions, described in the following lines, mainly because of the undetermined system of equations having fewer equations than unknowns.

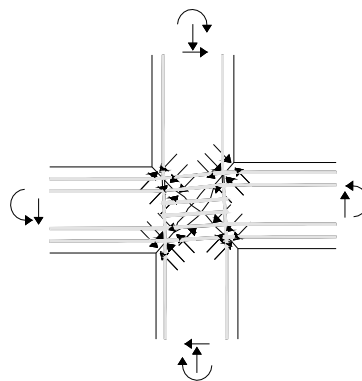


Figure 1. The basic scheme of original quadruple flexural resistance model (Shiohara [16]).

For instance in the interior joint, accounting for symmetry, given twelve equations defining equilibrium (three per rigid body), the number of independent equations representing the equilibrium reduces to five. Conversely, the unknowns are at least eight; three of them were assumed equal to experimental recorded data in experimental validation or directly assigned in the design phase. For instance yielding of joint stirrups was assumed (according to typical experimental outcomes after joint cracking) and also yielding of all beam bars, or alternatively yielding of tensile bars only and then the stress in compressed bars was derived by bond capacity limitation in the joint panel.

The model was also split to analyze potential beam failure or joint failure (evidently, beam column joint capacity is the smallest one of the two failure loads). However to avoid assuming *a priori* many unknowns, either supplied by experimental outcomes or considered at their maximum capacity (e.g., steel at yielding point, which actually is not always yielded at joint failure, when looking at experimental databases), modified unknowns, altered assumptions, and different solutions are herein proposed.

The basic idea is to include the beam mode into a unified joint model (adding apart a separate check not only of beam flexural failure, but also of column flexural failure, and for both, checking shear failure also). Doing so, it is possible to merge concrete compression and steel compression in a single compression force resultant at both beam and column ends. This assumption to merge compression in concrete and steel reinforcement has almost no effect on equilibrium of beams, while has minor effect

on columns where neutral axis is deeper (Cosenza *et al.*) [19]. Finally, considering column shear not as an unknown, but as the main driving parameter to study, it is possible to plot the evolution of all other internal force unknowns with the column shear, V_c , and to match the number of equations and unknowns. In this way, according to basic capacity design principles, column shear capacity is provided for each failure mode (e.g., column shear corresponding to concrete compression failure, is found on the curve of concrete in compression at a certain column shear value, V_c , intersecting concrete capacity; similarly column shear, V_c , corresponding to bond failure, is found on the bond demand curve while intersecting the bond capacity threshold). The model has been particularized for internal joints.

3.1. Mathematical Formulation

Joint scheme has been identified by setting geometric parameters and stresses, as shown in Figure 2. It is enough to analyze a single load direction, since load reversal yields to the same stress state, because of the symmetry of the joint. Symmetry of the beam column joint is obvious if the joint is exactly at $L_b/2$ and $L_c/2$, as it is usually in experimental and design schemes; however, this does not mean that steel reinforcement bars having as resultant force, T_1 , at the bottom of the right beam and at the top of the left beam have equal cross section or total area. Internal joints present a symmetry in terms of internal and external forces, but not necessarily in terms of reinforcement bars. Force resultants, F_i , (e.g., for the depicted case of clockwise moments on columns, F_1 and F_2 are in compression) are also shown in Figure 2. Accounting for symmetry, the number of nonlinear independent equations is five, in five unknowns (C , F_1 , F_2 , F_3 and F_4):

$$F_1 + F_4 - C \cdot \sin \vartheta - V_c = 0 \quad (1)$$

$$F_1 - F_4 - F_9 + C \cdot \sin \vartheta - N_b = 0 \quad (2)$$

$$F_2 - F_3 - F_{10} + C \cdot \cos \vartheta - N_c = 0 \quad (3)$$

$$F_2 + F_3 - C \cdot \cos \vartheta - \alpha \cdot V_c = 0 \quad (4)$$

$$h_b^* \cdot (F_1 + F_4) + h_c^* \cdot (F_2 + F_3) - \frac{C^2}{f_c \cdot B} - L_c \cdot V_c = 0 \quad (5)$$

Furthermore in this system, column and beam shear, V_c and V_b , as well as the flexural moment at column or beam, M_c or M_b , respectively, interface with joint satisfy also these relations:

$$V_c = \frac{(V_b \cdot L_b)}{L_c} \quad (6)$$

$$V_c = \frac{2 \cdot M_c}{(L_c - H_b)} \quad (7)$$

$$V_c = \frac{2 \cdot M_b \cdot L_b}{[(L_b - H_c) \cdot L_c]} \quad (8)$$

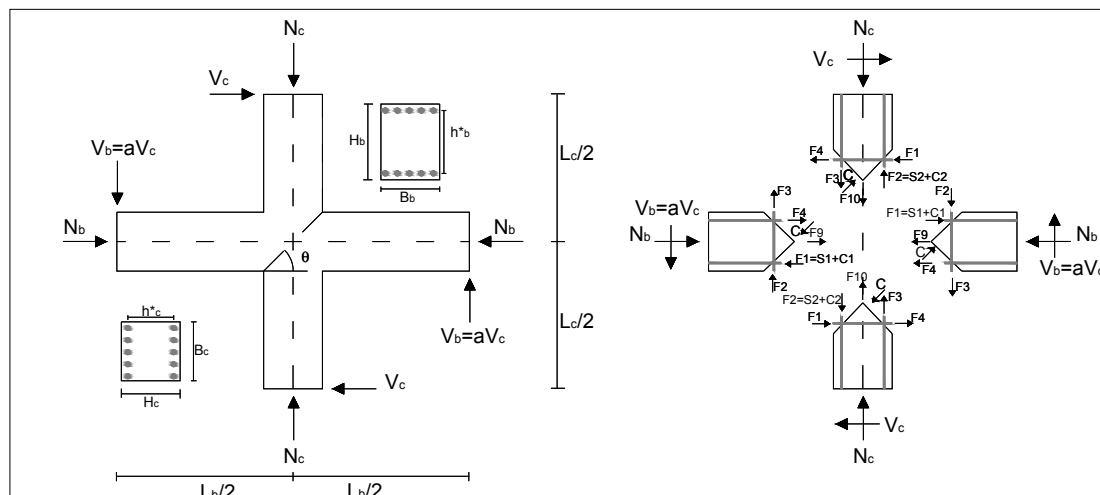


Figure 2. Internal perimetric joint: geometry, internal distribution of forces.

3.2. Failure Modes

The paper focuses on internal perimetric joint failure; however, to fully understand joint behavior, it is recommended to also evaluate beam and column peculiar failure modes (*i.e.*, flexural and shear capacity, according to classical structural analysis approaches, Cosenza *et al.* [19]). These failure modes are expressed in terms of column shear according to Equations (6)–(8), thus providing the first four possible column shear, V_c , capacity values corresponding to failure of the beam-column joint system. Eventual deficiencies of beams or columns in terms of flexural and shear capacities could be solved by means of FRP strengthening interventions, which are out of the scope of present paper and almost consolidated in the technical community.

Focusing on joint panel, three different failure modes can be expected: failure of concrete strut due to crushing, conventional failure due to yielding of longitudinal bars, or bond failure of longitudinal bars (in fact, the joint panel has limited dimensions to anchor the high stress demand and gradients from the bars).

The former failure mode involves the attainment of concrete crushing in the diagonal strut, so concrete contact force, C , should be limited to the compression strength of strut:

$$C_{max} = B \cdot f_c \cdot \frac{H_b}{2 \cdot \sin \theta} \tag{9}$$

If shear friction is assumed along cracks, the concrete contact force, C , can be assumed inclined not as the diagonal (*i.e.*, $\vartheta \neq \theta$), thus requiring a shear friction check where deviation from diagonal (*i.e.*, $|\vartheta - \theta|$) should be limited to a threshold value. Afterwards, conventional failure of reinforcement in tension is checked, assuming different bars at each longitudinal reinforcement level i , having cross section A_k , and yielding stress $f_{y,k}$. So each F_i should be limited to axial strength:

$$F_{max,i} = \sum A_k \cdot f_{y,k} \tag{10}$$

Finally, the latter failure mode requires splitting the compression resultant force into steel and concrete contributions (Figure 3). The basic idea is to evaluate (according to classical structural analysis

approaches, Cosenza *et al.* [19]) the neutral axis depth, recalling linearity of the strain diagram of the cross section; in the meantime, compression and tensile resultants are in equilibrium, according to the previous systems of equations.

Figure 3 also remembers that the neutral axis changes with increasing flexural loads due to concrete nonlinearity. The neutral axis, c , can be evaluated, for instance in the elastic field in a beam, without axial load, equating the first order moment to zero (Equation (11)) and, once the neutral axis, c , is known, the compressive force of reinforcements, S_1 , is derived:

$$B_b \cdot c^2 + n \cdot \left[A'_{s,b} \cdot (2 \cdot c - H_b + h_b^*) - A_{s,c} \cdot (H_b + h_b^* - 2 \cdot c) \right] = 0 \tag{11}$$

$$S_1 = F_4 \cdot \frac{A'_{s,c} \cdot (2 \cdot c - H_b + h_b^*)}{A_{s,b} \cdot (H_b + h_b^* - 2 \cdot c)} \tag{12}$$

Finally, estimating the effective bond length, L_{eb} , the upper bound bond capacity of concrete (based on uniform bond stress capacity, τ) is compared to the bond demand, given by the anchoring of longitudinal bars, even with different longitudinal diameters, Φ_k , of bars at the same level, e.g., due to the two resultants $S_1 + F_4$:

$$L_{eb} = \frac{h_b^*}{\tan \theta} \tag{13}$$

$$(S_1 + F_4)_{max} = \tau \cdot \sum L_{eb,k} \cdot \Phi_k \tag{14}$$

Three different bond stress capacities were considered according to Model Code 90 [20]: the maximum bond capacity, τ_{max} , is equal to $2.5 \cdot \sqrt{f_c}$ (good bond) or a medium value, τ_{med} is equal to $1.25 \cdot \sqrt{f_c}$ all others conditions) for ribbed bars. The minimum value, τ_{min} , equal to $0.3 \cdot \sqrt{f_c}$ can be used in the case of smooth bars. Different bond capacities' detailed analysis is out of the scope of present work, however they can be evaluated and inserted in the proposed model as bond capacity thresholds, e.g., $(S_1 + F_4)_{max}$, to estimate corresponding column shear, V_c .

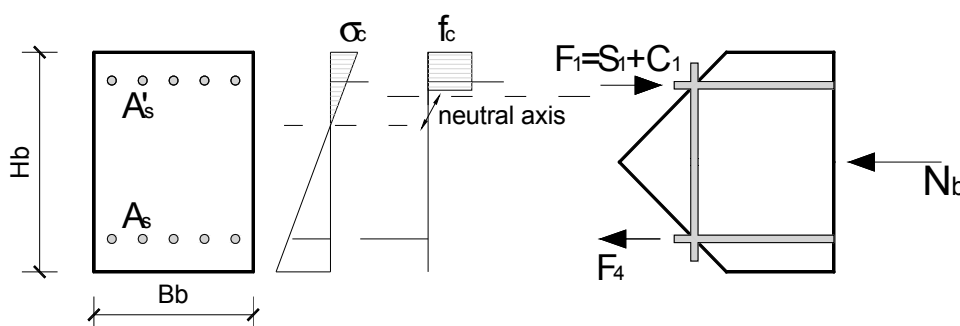


Figure 3. Analysis of distribution of compressive forces in concrete and reinforcement bars.

4. Behavior of Proposed Simplified Model

To evaluate the behavior of proposed simplified model, a parametric analysis is performed, on an internal perimetric joint, to highlight the peculiarities of this joint.

The joint analyzed to perform the parametric analysis is made of a beam of dimensions (30 cm \times 50 cm, increased in a case) and a column 30 cm \times 30 cm. The considered beam has length

equal to 3.60 m, reinforced by five D16 longitudinal bars at upper side and three D16 at the lower one. The length of the column is $L_c = 3.40$ m, reinforced symmetrically by two D16 longitudinal bars at upper and lower sides. Both of them have been transversally reinforced by using D8 stirrups (two legs) at 20 cm. Concrete cover value considered for both beam and column is 2.6 cm (see Figure 4).

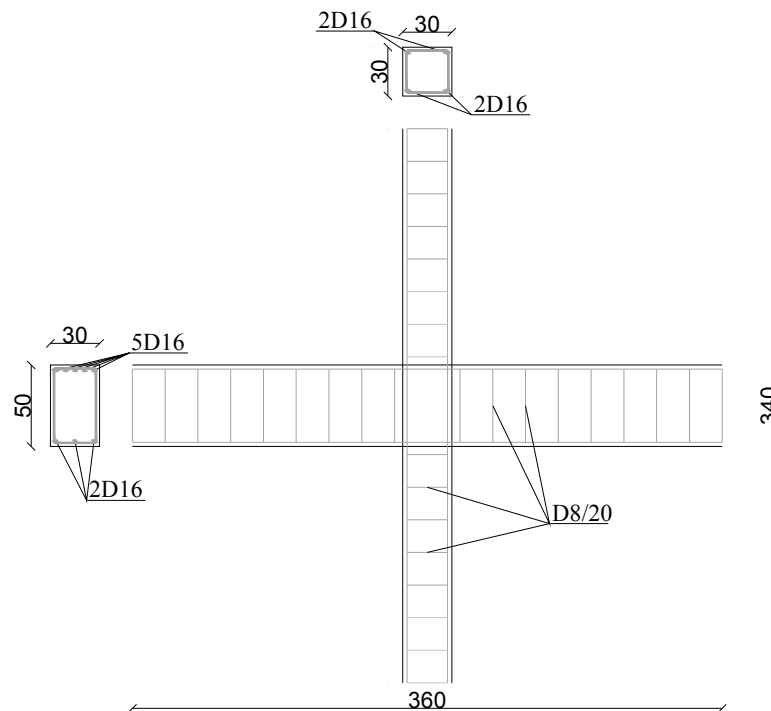


Figure 4. Geometry and reinforcement of analyzed beam column joint.

Scientific literature presents numerous experimental test results, conducted on different kinds of geometry, evaluating stress values leading to joint failure. By using the proposed model, for each geometry, the values of column shear, V_c , have been calculated for each of the failure modes for nodes (and named V_{c1} to V_{c11} for each considered failure mode, see Table 1). Starting from the reference condition, geometric variations have been performed leading to new column shear results related to each of the failure modes. In particular, variations about the number (two and four) of legs for stirrups and about the number and type of FRP layers have been considered. Four different Carbon CFRP (Young's modulus $E_f = 230$ GPa) configurations have been considered: one horizontal uni-axial layer ($t_f = 0.333$ mm), one quadri-axial layer, two quadri-axial layers, and four quadri-axial layers (each layer of quadri-axial has a thickness of 0.053 mm, hence combining the overlapping of inclined layer it is equivalent to 0.1279 mm in horizontal and vertical directions). FRP strain is assumed equal to debonding value (e.g., 0.4% according to Italian guidelines CNR DT200 R1 2013 [21]).

In order to understand which failure mode is independent from the reinforcement and which is improvable by using reinforcement, results were grouped and compared to the reference case, to represent values of column shear (for each failure mode) related to the amount of reinforcement. The main considered parameters were: axial load on column, N_c ; concrete strength, f_c ; stirrups in the joint; FRP externally bonded on the joint panel; longitudinal reinforcement ratio in beams and columns; and beam height, hence joint panel dimensions. Variability of considered parameters is depicted in a

numerical test matrix (in Table 2 at every case is associated an ID number). The identification of the failure mode allowed to establish if and how it is possible to change and improve the hierarchy of the failure modes. In many cases, the method led to switch a brittle failure mode into ductile failure modes, even if some mechanisms are independent from the reinforcement inserted into the joint.

Table 1. Column shear, V_c , for each considered failure mode.

Column Shear	Failure mode
V_{c1}	Bending capacity of beam
V_{c2}	Bending capacity of column
V_{c3}	Shear capacity of beam
V_{c4}	Shear capacity of column
V_{c5}	Joint with yielding of bars of beam
V_{c6}	Joint with yielding of bars of column
V_{c8}	Joint due to maximum bond exceedance
V_{c9}	Joint due to medium bond exceedance
V_{c10}	Joint due to minimum bond exceedance
V_{c11}	Joint due to concrete strut crushing

Table 2. Parametric analysis: variability of considered parameters; failure modes and column shear capacities of considered joint configurations.

ID number	N_c (kN)	f_c (MPa)	Stirrups	FRP	Beam dimension (cm ²)	Failure mode (kN)
1	0	20	-	-	(50 × 30)	Vc2 37.14
2	315	20	-	-	(50 × 30)	Vc5 55.91
3	630	20	-	-	(50 × 30)	Vc5 55.91
4	315	40	-	-	(50 × 30)	Vc5 59.01
5	315	60	-	-	(50 × 30)	Vc5 60.03
6	315	20	2D8	-	(50 × 30)	Vc2 62.18
7	315	20	4D8	-	(50 × 30)	Vc2 62.18
8	315	20	8D8	-	(50 × 30)	Vc2 62.18
9	315	20	-	1 ply ^{quadi-axial}	(50 × 30)	Vc5 60.51
10	315	20	-	1 ply ^{uni-axial}	(50 × 30)	Vc2 62.18
11	315	20	-	2 plies ^{quadi-axial}	(50 × 30)	Vc2 62.18
12	315	20	-	4 plies ^{quadi-axial}	(50 × 30)	Vc2 62.18
13	315	20	-	-	(70 × 30)	Vc2 66.79
14 ¹	315	20	-	-	(50 × 30)	Vc2 62.18
15 ²	315	20	-	-	(50 × 30)	Vc8 20.08

$$^1 \theta - \vartheta = +20^\circ; ^2 \theta + \vartheta = -20^\circ.$$

As expected, those are all the mechanisms external to the joint (e.g., failure for bending and shear of column or beam) not incorporated in the system of equations previously presented. Furthermore, thanks to the symmetry of the joint, the values for yield strength in upper and lower bars of the column are the same for each analysis (for this reason V_{c7} was omitted because it is equal to V_{c6}).

It is clear from Table 1 that in the case of zero axial load on column (ID1), the failure of the system is due to the flexural failure of column in bending (*i.e.*, $V_{c2} = 37.14$ kN is the lower column shear triggering the failure mode). Increasing the axial load (ID2 and ID3) the failure moves to the joint due to yielding

of bars in beam (*i.e.*, $V_{c5} = 55.91$ kN is the lower column shear triggering the failure mode). The increase of concrete strength (ID4 and ID5) simply increases slightly the column shear leading to the same failure mode of the joint.

Any improvement of the joint reinforcement (ID6 to ID8 in the case of internal reinforcement of new structures, or ID9 to ID12 in the case of external retrofit of existing structures) moves the failure mode from the brittle failure of the joint due to yielding of bars in the beam to the flexural failure of the column. Only an exception is represented by one ply of quadri-axial reinforcement (ID9), not sufficient in the horizontal direction to avoid a joint failure due to yielding of beam bars at a slightly lower load. Increasing the dimensions of the joints (ID13) allows preventing of joint failure, hence moving to the flexural failure of the column (at a slightly higher load, not because joint dimensions increase the ultimate moment of the column, but because the lever arms slightly changes; see Equation (7)).

Assuming a friction along the diagonal cracks in the joint (ID14 and ID15 and assuming the maximum of both) improves slightly the capacity of the joint pushing failure to the flexural capacity of the column.

Since the flexural failure of the column is not yet the optimum failure mode, a further intervention could be foreseen for the column, hence increasing the flexural capacity up to a switch of the failure mode to the beam flexural failure, the optimal ductile failure of such systems. It is worth noting that once increasing the flexural capacity of a member, in this case the column, a shear check should always be coupled and performed to evaluate the need for a combined shear strengthening, because shear loads on the member could increase with the flexural improvement. However this latter aspect of column strengthening is out of the scope of present work.

This discussion was performed assuming a good bond condition. However, in the case of smooth bars, with poor bond conditions, the failure mode would always occur at a much lower column shear with joint failure due to the bond of the longitudinal bars inside the joint. The fifteen analyses (Tables 2 and 3) allow assessing the influence of different parameters, both in terms of failure mode and column shear, V_c . In some cases, a parameter has no influence on the effective failure mode, however it has an influence on other possible failure modes, but not triggered first in that case. The effect of axial load is mainly on column reinforcement forces and flexural and shear capacity (see Figure 5 where the force resultant F_3 reaches its yielding value at increasing column shear, V_c , when increasing axial load on column, N_c). In Figure 5, $F_3(V_c)$ curves have different origins because the higher is the axial load, N_c , the higher is initial compression level at zero lateral load, V_c . Similarly, column shear corresponding to column flexural failure increases from 37.14 kN to 79.46 kN (+114%) (in square brackets the percentage increase has been reported), yet not being triggered as the first failure mode. Axial load has negligible effect on joint failure. The effect of concrete strength is mainly related to shear and flexural capacity of beams and columns.

A clear effect is also on bond capacity; Figure 6 shows bond demand $F_4 + S_1$ reaching its capacity value at increasing column shear, V_c , when changing bond capacity (in good bond conditions) due to concrete strength $\tau_{\max}(f_c)$.

To evaluate the failure mode for each considered configuration case it is possible to refer to values reported in Table 3.

Table 3. Column shear for each configuration case and for every failure mode (to evaluate the strength hierarchy).

Column shear at failure	Configuration ID Number														
	1	2	3	4	5	6	7	8	9	10	11	12	13	14	15
V_{c1} (kN)	91.4	91.4	91.4	92.7	93.8	91.4	91.4	91.4	91.4	91.4	91.4	91.4	132.5	91.4	91.4
V_{c2} (kN)	37.1	62.2	79.5	65.2	66.9	62.2	62.2	62.2	62.2	62.2	62.2	62.2	66.8	62.2	62.2
V_{c3} (kN)	295.0	295.0	295.0	295.0	295.0	295.0	295.0	295.0	295.0	295.0	295.0	295.0	419.5	295.0	295.0
V_{c4} (kN)	161.1	161.1	161.1	161.1	161.1	161.1	161.1	161.1	161.1	161.1	161.1	161.1	161.1	161.1	161.1
V_{c5} (kN)	55.9	55.9	55.9	59.0	60.0	64.0	71.7	86.1	60.5	67.7	65.00	73.6	78.6	65.7	47.5
V_{c6} (kN)	58.7	93.8	120.4	104.4	107.8	93.8	93.8	93.8	97.4	93.8	100.5	106.8	177.2	64.0	106.9
V_{c8} (kN)	67.2	67.2	67.2	99.1	123.5	74.8	82.1	95.4	71.6	78.2	75.8	83.8	104.4	120.5	20.1
V_{c9} (kN)	36.0	36.0	36.0	51.9	64.1	44.9	53.5	69.5	41.1	48.9	46.0	55.6	53.6	79.7	10.2
V_{c10} (kN)	9.1	9.1	9.1	12.9	15.8	18.9	28.5	46.5	14.7	23.4	20.2	30.8	13.1	22.4	2.5
V_{c11} (kN)	144.5	144.5	144.5	289.0	433.6	144.5	144.5	144.5	144.5	144.5	144.5	144.5	144.5	124.2	130.8

Bold values refer to triggered failure mode with maximum bond conditions; V_{c8} , τ_{max} is $2.5 \cdot \sqrt{f_c}$; V_{c9} , τ_{med} is $1.25 \cdot \sqrt{f_c}$; V_{c10} , τ_{min} is $0.3 \cdot \sqrt{f_c}$.

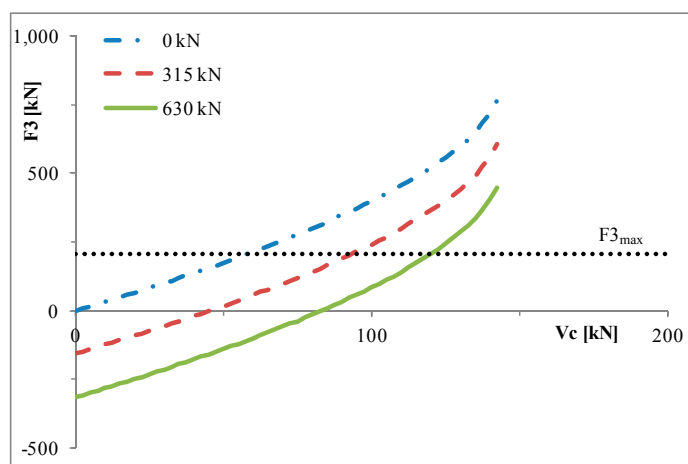


Figure 5. Parametric analysis: tensile force, F_3 , in column bars and its threshold with variability of axial load, N_c .

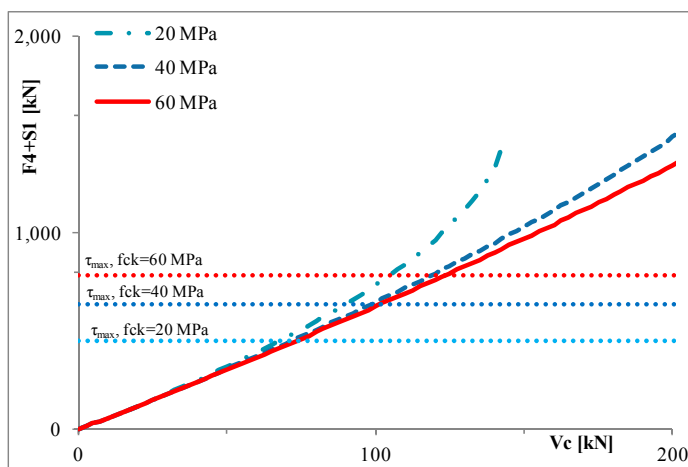


Figure 6. Parametric analysis: Bond demand of beam bars, $F_4 + S_1$, and its threshold with variability of concrete strength, f_c .

The effect of stirrups is meaningful, as it has many consequences. The most relevant is on longitudinal reinforcement bars, reducing their load, thus bearing a portion of horizontal load demand. Stirrups are assumed to yield, and for simplicity, their tensile force (T_9) is assumed equal to yielding force from the very beginning; for this reason, in Figure 7 the $F_4(V_c)$ curves have different origins. However the presence of stirrups increases column shear corresponding to joint failure due to beam tensile reinforcement yielding from 55.91 kN (no stirrups and actual failure of ID2 case) to 64.01 kN (+14.48%) (two D8 stirrups with two legs, ID6 case) and 86.14 kN (+54.06%) (eight D8 stirrups with two legs), but in these cases the failure mode switches to column flexural failure. Thus, it can be concluded that, in this case, two D8 stirrups are enough to change the failure mode from brittle joint failure to more desirable ductile column flexural failure.

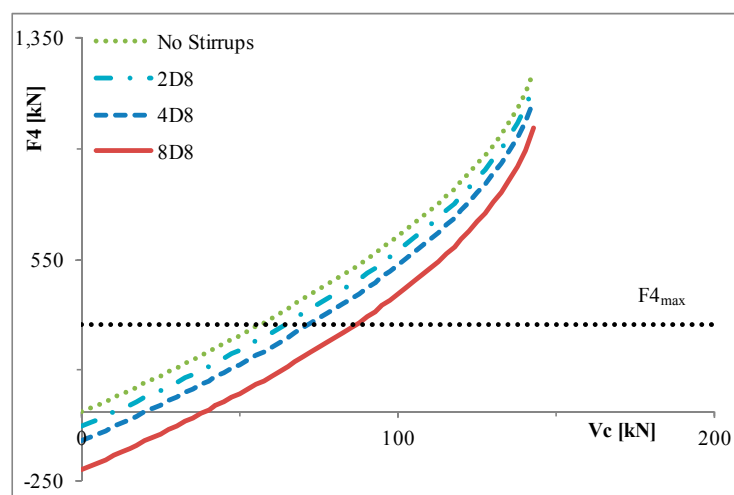


Figure 7. Parametric analysis: tensile force, F_4 , in beam bars and its threshold with variability of stirrups.

Similar comments can be repeated for externally-bonded FRP. The role of the reinforcement is similar to the insertion of stirrups; however, benefits can also be achieved on an existing joint, even if, originally, they have no internal stirrups. From a numerical point of view, the presence of FRP is similar to stirrups (note that one ply of uni-axial FRP is not enough to change the failure mode, remaining the joint failure with yielding of beam bars). FRP and stirrups both provide an increase of horizontal, T_9 , (or vertical, T_{10} , if vertical fibers are also applied) load carrying capacity. FRP tensile force is assumed equal to the debonding force from the very beginning. For this reason, in Figure 8 the $F_4(V_c)$ curves have different origins. However, the presence of FRP increases the shear column value, V_c , corresponding to system failure, from 55.91 kN (yet joint failure due to beam tensile reinforcement yielding) to 65.00 kN (+16.25%) (two plies of quadri-axial FRP, ID11 case). FRP was able to change the failure mode from brittle joint failure to more desirable ductile column flexural failure, with the only exception of ID9.

Longitudinal reinforcement has a low influence on the evaluation of force resultants, e.g., Figure 9 shows the $F_4(V_c)$ curves, they are overlapping; however, the yielding capacity is different, thus leading to much different column shear values, V_c , corresponding to joint failure due to beam tensile reinforcement yielding. These column shear values, V_c , reduces from 55.91 kN (actual failure of ID2 case) to 38.66 kN (−30.85%) (2+2D16 bars in the beams), or increases to 144.53 kN (+158.5%) (4+4D32 bars in the

beams) yet not reaching yielding of bars, however in this latter case the failure mode is a different one, the column flexural failure, at $V_c = 62.18$ kN. Conversely, the increase of beam dimensions has two main effects: the first one is the increase of beam capacity, both in terms of flexure and shear; and the second one is the increase of joint panel dimensions.

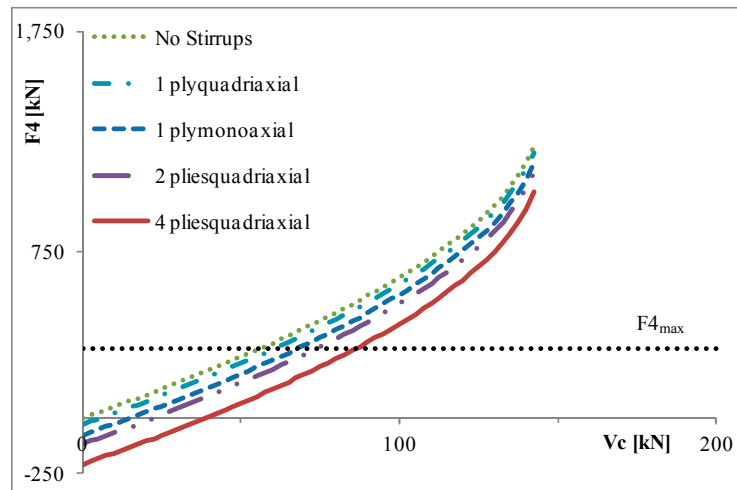


Figure 8. Parametric analysis: tensile force, F_4 , in beam bars and its threshold with variability of externally bonded FRP.

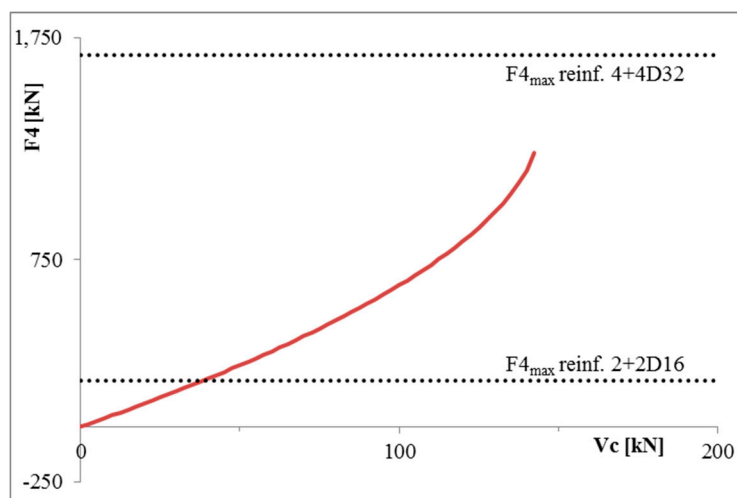


Figure 9. Parametric analysis: tensile force, F_4 , in beam bars and its threshold with variability of longitudinal beam reinforcement.

The increase of joint panel dimensions reduces the demand in terms of resultant forces in reinforcements, as shown in Figure 10 where the bond demand is lower for the higher beam. The same figure also highlights the influence of bond capacity: the same beam-column joint, if reinforced with smooth bars, presents a much lower capacity. In the case of beams of dimensions $70\text{ cm} \times 30\text{ cm}$, potential failure due to bond occurs at 97.45 kN in the case of good bond for ribbed bars, and it drops dramatically to 12.62 kN (-87.05%) in the case of smooth bars. It is a “potential” failure mode in the case of a good bond with ribbed bars, because the actual failure mode is column flexural failure at a shear column value, $V_c = 66.79$ kN.

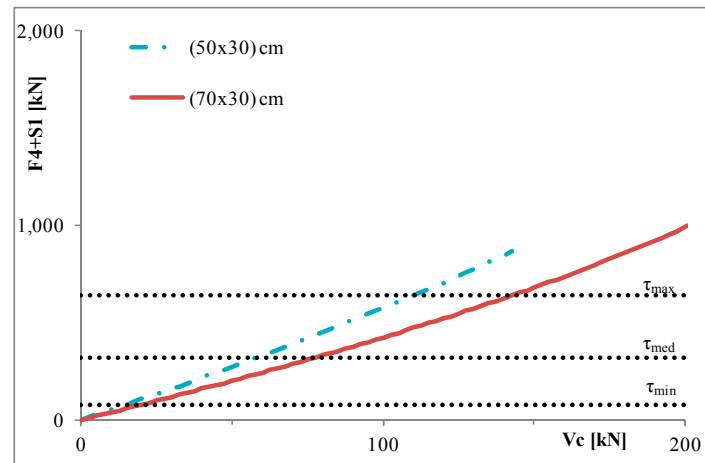


Figure 10. Parametric analysis: tensile force, F_4 , in beam bars and its threshold with variability of longitudinal beam reinforcement.

Compared to counterpart case ID2 (differing only for beam height), the increase of joint panel dimensions increases the failure load. Conversely, if smooth bars were used, the predicted failure mode of the system would have occurred due to bond failure at a very low shear column value, $V_c = 12.62$ kN. This leads one to conclude that bond capacity has a meaningful effect on beam-column joint strength.

5. Model Validation

Theoretical predictions of the proposed simplified model were also compared to some experimental tests available in the literature (Hakuto *et al.* [22], Prota *et al.* [23] and Zaid *et al.* [24]) to validate the proposed theoretical model. Following, some beam-column joint specimens will be discussed in detail showing the entire table of “potential” failure modes. Actual failure load is the smallest of the potential failure modes. Discussion of the results considers two limit bond performances: maximum and minimum (due to smooth bars) bond conditions. This approach allows one not only to better understand the strength hierarchy, but also to calibrate strengthening design.

The basic idea is to avoid all undesired failure modes (e.g., brittle shear failure of joint, but also of beams and columns) to push failure mode to more desirable ductile beam flexural failure. Once the desired failure mode is selected, than all failure mode mechanisms presenting lower column shear values should be improved and strengthening (on existing structures) or design improvements (in structures still under design) can be calibrated to exceed the column shear, V_c corresponding to desired failure mode (*i.e.*, according to “capacity design” approach).

Six retrofit configurations have been implemented, and “applied” to literature experimental results. In particular they have been supposed (as retrofit method): (a) one quadri-axial ply of FRP of thickness, $t = 0.1279$ mm; (b) two quadri-axial plies of FRP of thickness, $t = 0.2559$ mm; (c) four quadri-axial plies of FRP of thickness, $t = 0.5116$ mm; (d) one uni-axial horizontal ply of FRP of thickness, $t = 0.333$ mm; (e) two stirrups (two legs) of diameter 12 mm; and (f) four stirrups (two legs) of diameter 12 mm, simulated into the model by appropriate values of F_9 and F_{10} .

In all the cases FRP has a Young’s Modulus of 230 GPa and is assumed to debond at 0.4%. Table 4 shows concrete characteristics and beam and column longitudinal and transversal reinforcements for all considered specimens of experimental tests available in scientific literature.

Table 4. Geometrical and mechanical properties of specimens of experimental programs.

Specimen ID Number	Concrete characteristics		Concrete section		Concrete cover		Beam						Column						Stirrups			
	N_c	f_{ck}	Beam	Column	Beam	Column	Upper side			Lower side			Upper side			Lower side			Beam		Column	
							Bar diameter	$A'_{s,b}$	f_y	Bar diameter	$A_{s,b}$	f_y	Bar diameter	$A'_{s,c}$	f_y	Bar diameter	$A_{s,c}$	f_y	legs, diameter	f_y	legs, diameter	f_y
kN	MPa	cm ²	cm ²	mm	mm	mm	cm ²	MPa	mm	cm ²	MPa	mm	cm ²	MPa	mm	cm ²	MPa	N ^o , mm	MPa	N ^o , mm	MPa	
Hakuto et al. [22]																						
Unit 5	0	33	50 × 30	46 × 46	36	40	32	16.08	306	32	16.08	306	28	18.46	321	28	18.46	321	2, 12	398	2, 12	398
Unit 1	0	41	50 × 30	46 × 30	40	40	24	9.04	325	24	18.09	325	24	13.56	325	24	13.56	325	2, 12	399	4, 12	399
Prota et al. [23]																						
L1	124.5	38.6	35.5 × 20	20 × 20	38	38	22	11.40	599	18	5.08	511	16	8.04	449	16	8.04	449	2, 12	398	2, 12	398
H1	249.0	31.7																				
L2	124.5	39.8																				
H2	249.0	36.5																				
Zaid et al. [24]																						
1	100	28	30 × 20	30 × 30	35	35	16	10.05	470	16	10.05	470	19	11.34	450	19	11.34	450	1, 6	390	1, 6	390

However more details about experimental programs and results can be found in relevant cited publications. Table 5 shows results obtained by the resolution of the experimental configuration model (for each experimental program and each specimen).

The validation is proposed in Table 6 where the agreement between experimental outcomes and model predictions (both in terms of failure modes and column shear capacity) is usually satisfactory and on the safe side.

Table 5. Theoretical prediction of capacities for each potential failure modes of specimens of experimental programs.

Column shear at failure	Experimental program						
	Hakuto <i>et al.</i> [22]		Prota <i>et al.</i> [23]				Zaid <i>et al.</i> [24]
	Unit 05	Unit 01	L1	H1	L2	H2	Specimen 3
V_{c1} (kN)	170.50	94.32	63.20	62.43	63.29	62.95	171.26
V_{c2} (kN)	197.57	131.17	32.50	36.73	33.82	40.67	228.73
V_{c3} (kN)	299.21	248.54	32.57	434.84	501.26	475.32	446.75
V_{c4} (kN)	739.40	629.79	128.76	128.76	247.56	244.56	328.58
V_{c5} (kN)	130.19	76.03	35.90	32.26	33.31	32.94	121.52
V_{c6} (kN)	163.44	121.55	53.07	54.34	49.49	57.20	128.33
V_{c8} (kN)	192.62	187.06	30.19	26.93	30.58	29.14	129.80
V_{c9} (kN)	111.22	99.95	15.93	14.30	16.12	15.41	90.91
V_{c10} (kN)	<i>29.22</i>	<i>25.12</i>	<i>3.97</i>	<i>3.58</i>	<i>4.02</i>	<i>3.85</i>	<i>36.01</i>
V_{c11} (kN)	250.39	400.84	79.73	64.97	81.58	74.81	132.87

Bold numbers indicate failure considering maximum bond. Italic numbers indicate failure considering minimum bond.

Table 6. General validation of model by means of comparison of experimental outcomes and simplified model predictions.

Reference and Specimen ID	Experimental		Theoretical		Difference %
	Failure mode	V_c (kN)	Failure mode	V_c (kN)	
Hakuto <i>et al.</i> [22] O1	J	89.0	J	76.0	-15%
Hakuto <i>et al.</i> [22] O5	BS	150.0	J	130.2	-13%
Prota <i>et al.</i> [23] L1	CF	32.7	CF	32.5	-1%
Prota <i>et al.</i> [23] H1	CF	37.7	J	32.3	-14%
Prota <i>et al.</i> [23] L2	CF	31.6	CF	33.3	5%
Prota <i>et al.</i> [23] H2	J	38.4	J	32.9	-14%
Zaid <i>et al.</i> [24] S3	J	130.0	J	121.5	-6%

(J) is joint failure due to beam tensile reinforcement yielding; (CF) is column flexural failure; (BS) is beam shear failure.

5.1. Simulation of Experimental Tests in Research from Hakuto et al.

Both specimens tested by Hakuto et al. [22], have a failure mode due to yielding of bars of the beam, with a value of V_{c5} equal to 130.20 kN and 76.03 kN, for Unit 5 and Unit 1 (considering maximum bond), respectively. The proposed model satisfactorily underestimates the actual capacity of the tested joint. By applying the retrofit methods (a) to (d) at Unit 5, the failure mode does not change (both in case of minimum or maximum bond); instead, applying methods (e) and (f), the failure mode in case of maximum bond, moves from yielding of bars of column to yielding of bars of column, but not one of the considered retrofits provides a ductile failure mode. Unit 1 has a different behavior. Considering the maximum bond case, by applying the retrofit methods (a) and (b) failure does not change. In case of maximum bond, retrofit methods (c) to (f) allow to move to a failure mode due to bending moment of the beam (the most desirable one) applying three plies of FRP ($t = 0.33$ mm), so the joint is upgradable. Results of the specimen named Unit 1 are shown in Table 7.

Table 7. General validation of model by means of comparison of experimental outcomes and simplified model predictions.

Column shear at failure	Hakuto et al.—Unit 01						
	No retrofit	1 ply (a)	2 plies (b)	4 plies (c)	1 Uni-axial ply (d)	2 Stirrups (e)	4 Stirrups (f)
V_{c1} (kN)	94.32	94.32	94.32	94.32	94.32	94.32	94.32
V_{c2} (kN)	131.17	131.17	131.17	131.17	131.17	131.17	131.17
V_{c3} (kN)	248.54	248.54	248.54	248.54	248.54	248.54	248.54
V_{c4} (kN)	629.79	629.79	629.79	629.79	629.79	629.79	629.79
V_{c5} (kN)	76.03	83.26	90.41	104.51	94.69	112.91	147.80
V_{c6} (kN)	121.55	128.38	135.14	148.41	121.56	121.56	121.56
V_{c8} (kN)	187.06	193.05	198.97	210.57	202.50	217.45	245.72
V_{c9} (kN)	99.95	106.94	113.85	127.46	117.98	135.56	169.16
V_{c10} (kN)	25.12	32.83	40.46	55.52	45.03	64.50	101.97
V_{c11} (kN)	400.84	400.84	400.84	400.84	400.84	400.84	400.84

Bold numbers indicate failure considering maximum bond. Italic numbers indicate failure considering minimum bond.

5.2. Simulation of Experimental Tests in Research from Prota et al.

In this paper [23], four specimens of a wider experimental program on perimeteric joints have been considered, namely H1, L1, L2, and H2. For all of them, column length, L_c , is 264 cm, beam length, L_b , is 305 cm, distance between reinforcement layers in the column, $h_c^* = 12.4$ cm, distance between reinforcement layers in the beam, $h_b^* = 27.9$ cm, and concrete cover of beam and column is 4 cm.

The specimen named L1 does not present external FRP reinforcement. Considering the case of maximum bond the failure mode can be changed by applying one ply of uni-axial FRP ($t = 0.13$ mm) from bond failure to the bending moment of the column. Similar results can be obtained in cases of medium or minimum bond, increasing the number of FRP plies or the number of stirrups. In any case, the retrofit yields to a failure due to the bending moment of the column. Nevertheless, to avoid this kind of joint failure, column bending capacity needs to be improved, but this kind of retrofit is out of the scope of present paper. Results are shown in Table 8.

Concrete strength of specimen H1 (31.70 MPa) and H2 (36.50 MPa) is lower than previous cases (specimen L1 $f_c = 38.60$ MPa), so it is more difficult to obtain every desirable failure mode.

Considering maximum bond, the failure mode moves to flexural column failure by application of retrofit named (f) in both cases, even if V_c values of specimen H2 are higher than values of specimen H1. Furthermore, the reduced concrete strength reduces the possibilities of FRP retrofit since the concrete strut crushing (*i.e.*, V_{c11}) could occur at column shear close to the desired flexural failure of beams (*i.e.*, V_{c1}). All potential failure modes and relevant column shears are reported in Tables 9 and 10.

Specimen L2 presents results comparable with specimen L1.

Table 8. Theoretical prediction of capacities for each potential failure modes of different retrofit solutions for specimens “L1” (Prota *et al.*).

Column shear at failure	Prota <i>et al.</i> —L1						
	No retrofit	1 ply (a)	2 plies (b)	4 plies (c)	1 uni-axial ply (d)	2 Stirrups (e)	4 Stirrups (f)
V_{c1} (kN)	63.20	63.20	63.20	63.20	63.20	63.20	63.20
V_{c2} (kN)	32.57	32.57	32.57	32.57	32.57	32.57	32.57
V_{c3} (kN)	494.32	494.32	494.32	494.32	494.32	494.32	494.32
V_{c4} (kN)	128.76	128.76	128.76	128.76	128.76	128.76	128.76
V_{c5} (kN)	35.90	38.15	40.33	44.53	41.62	43.25	49.96
V_{c6} (kN)	53.07	54.78	56.45	59.62	53.06	53.07	53.07
V_{c8} (kN)	30.19	32.57	34.89	39.36	36.26	38.00	45.18
V_{c9} (kN)	15.93	18.61	21.24	26.33	22.79	24.78	33.00
V_{c10} (kN)	3.97	6.88	9.73	15.28	11.42	13.59	22.59
V_{c11} (kN)	79.73	79.73	79.73	79.73	79.73	79.73	79.73

Bold numbers indicate failure considering maximum bond. Italic numbers indicate failure considering minimum bond.

Table 9. Theoretical prediction of capacities for each potential failure modes of different retrofit solutions for specimens “H1” (Prota *et al.*).

Column shear at failure	Prota <i>et al.</i> —H1						
	No retrofit	1 ply (a)	2 plies (b)	4 plies (c)	1 uni-axial ply (d)	2 Stirrups (e)	4 Stirrups (f)
V_{c1} (kN)	62.43	62.43	62.43	62.43	62.43	62.43	62.43
V_{c2} (kN)	36.73	36.73	36.73	36.73	36.73	36.73	36.73
V_{c3} (kN)	434.84	434.84	434.84	434.84	434.84	434.84	434.84
V_{c4} (kN)	128.76	128.76	128.76	128.76	128.76	128.76	128.76
V_{c5} (kN)	32.26	34.40	36.47	40.41	37.69	39.22	45.39
V_{c6} (kN)	54.34	55.54	56.68	58.75	54.32	54.34	54.34
V_{c8} (kN)	26.93	29.23	31.47	35.73	32.78	34.44	41.17
V_{c9} (kN)	14.30	16.94	19.52	24.47	21.04	22.96	30.86
V_{c10} (kN)	3.58	6.47	9.30	14.76	10.97	13.10	21.87
V_{c11} (kN)	64.97	64.97	64.97	64.97	64.97	64.97	64.97

Bold numbers indicate failure considering maximum bond. Italic numbers indicate failure considering minimum bond.

Table 10. Theoretical prediction of capacities for each potential failure modes of different retrofit solutions for specimens “H2” (Prota *et al.*).

Column shear at failure	Prota <i>et al.</i> —H2						
	No retrofit	1 ply (a)	2 plies (b)	4 plies (c)	1 uni-axial ply (d)	2 Stirrups (e)	4 Stirrups (f)
V_{c1} (kN)	62.95	62.95	62.95	62.95	62.95	62.95	62.95
V_{c2} (kN)	40.67	40.67	40.67	40.67	40.67	40.67	40.67
V_{c3} (kN)	475.32	475.32	475.32	475.32	475.32	475.32	475.32
V_{c4} (kN)	244.56	244.56	244.56	244.56	244.56	244.56	244.56
V_{c5} (kN)	32.94	35.20	37.40	41.61	38.69	40.34	47.05
V_{c6} (kN)	57.20	58.64	60.03	62.64	57.18	57.20	57.20
V_{c8} (kN)	29.14	31.50	33.79	38.20	35.15	36.86	43.91
V_{c9} (kN)	15.41	18.08	20.69	25.73	22.23	24.20	32.32
V_{c10} (kN)	3.85	6.75	9.59	<i>15.11</i>	<i>11.28</i>	<i>13.43</i>	22.37
V_{c11} (kN)	74.81	74.81	74.81	74.81	74.81	74.81	74.81

Bold numbers indicate failure considering maximum bond. Italic numbers indicate failure considering minimum bond.

5.3. Simulation of Experimental Tests in Research from Zaid *et al.*

In this case [24], column length, L_c , is 147 cm, beam length, L_b , is 270 cm, distance between reinforcements layer in the column, $h_c^* = 23$ cm, distance between reinforcements layer in the beam, $h_b^* = 23$ cm, concrete cover of beam and column is 3.5 cm and concrete contact force inclination is equal to $\vartheta = 0.785$ rad.

Results obtained by applying retrofits (a) to (f), and not reported here for brevity, show that it is not possible to move from the joint failure mode due to yielding of bars of beam by retrofitting the joint only with the considered retrofit configurations. In this case the reinforcement ratio of the beams is high; hence the flexural capacity is relatively high to move to the desired ductile flexural beam failure.

6. Concluding Remarks

The beam-column joints behavior can strongly influence the seismic performance of RC buildings. A simplified analytical/mechanical model of joint behavior is discussed and theoretical simulations are performed in order to fully understand the mechanical behavior and the failure modes. Compared to previous models and theories the proposed one does not require FEM or complex nonlinear numerical analyses of the structure or sub-assembly and does not require the calibration of empirical factors to account for the many parameters affecting joint seismic response and outlined in the paper.

The model moves from a previous one, but it improves and alters deeply the main unknowns, assumptions, and solutions. Among the main parameters affecting the performance of joints, namely material property, joint panel geometry, reinforcement in joint panel, column axial load, and reinforcement bond condition; axial load on columns showed negligible influence, while meaningful influence was given by bond performance. Similarly, joint (transverse) reinforcement, either external FRP or internal stirrups, provides many benefits pushing failure mode from brittle joint shear to ductile beam flexural.

The identification of the failure mode establishes if and how it is possible to change and improve the hierarchy of the failure modes to switch a brittle failure mode into ductile failure modes, even

if some mechanisms are independent from the reinforcement inserted into the joint, and should be treated independently.

Once the desired failure mode is selected, than all failure mode mechanisms presenting lower column shear values should be improved and strengthening (on existing structures) or design improvements (in structures still under design) can be calibrated to exceed the column shear, V_c corresponding to desired failure mode. Hence, the proposed tool fully fits the “capacity design” approach for strengthening interventions design.

Notation List

A_k : Longitudinal reinforcement cross section; $A'_{s,b}$: Section of bars of upper side of Beam; $A_{s,b}$: Section of bars of lower side of Beam; $A'_{s,c}$: Section of bars of upper side of Column; $A_{s,c}$: Section of bars of lower side of Column; B : Depth of the joint; B_b : Depth of the section of the beam; B_c : Depth of the section of the column; BF: Beam flexural failure; BS: Beam shear failure; c : The neutral axis; C : Concrete contact force; D : Diameter; f_c : Mean concrete compressive strength; f_y : Longitudinal reinforcement maximum stress; $f_{y,k}$: Longitudinal reinforcement yielding stress; F_i : Force resultants; h^*_b : Distance between reinforcements layer in a beam; h^*_c : Distance between reinforcements layer in a column; H_b : Height of the section of the beam; H_c : Height of the section of the column; i : Longitudinal reinforcement level; J: Joint failure; L_b : Length of beam; L_c : Length of column; L_{eb} : Effective bond length; M_b : Flexural moment of beam; M_c : Flexural moment of column; N_b : Axial load on beam; N_c : Axial load on column; n : Number of longitudinal bars; R_2 : Effective bond length; S_i : Reinforcement forces; T_i : Steel bars' resultant force; t : Thickness of FRP ply; V_b : Shear beam; V_c : Shear column; α : L_c/L_b ratio; θ : Diagonal of the joint panel inclination; ϑ : Concrete contact force inclination; σ_c : Compressive stress of concrete; τ : Uniform bond stress capacity; τ_{max} : Maximum bond capacity; τ_{med} : Medium bond capacity; τ_{min} : Minimum bond capacity; Φ_k : Longitudinal reinforcement diameter.

Conflicts of Interest

The authors declare no conflict of interest.

Appendix

In this appendix a numerical worked example is proposed analyzing the experimental test S3 by Zaid *et al.*, [24]. The main system of Equations (1) to (5) is solved adopting as input the geometrical parameters and material characteristics reported in the last line of Table 4 for the relevant experimental S3 data of Zaid *et al.*, [24]. $F_9 = 88.22$ kN is the capacity of the 4 stirrups (2 legs D6) in the joint. In this way it is possible to calculate the main five unknowns $F_i(V_c)$ [N], with i equal to 1 to 4 and diagonal contact force $C(V_c)$ [N].

$$F_1 = 0.5 \times 91,908 + V_c \quad (1A)$$

$$F_2 = 5.56 \times 10^{-3} \times (9,000,000 + 49 \cdot V_c) \quad (2A)$$

$$F_3 = 1.41 \times 10^{-27} \times (4.20 \times 10^{32} - 9.80 \times 10^{11} \times \sqrt{2.16 \times 10^{41} - 1.63 \times 10^{36} \cdot V_c} + 1.92 \times 10^{26} \cdot V_c) \quad (3A)$$

$$F_4 = 8.38 \times 10^{-25} \times (7.13 \times 10^{29} - 1.65 \times 10^9 \times \sqrt{2.16 \times 10^{41} - 1.63 \times 10^{36} \cdot V_c} + 5.97 \times 10^{23} \cdot V_c) \quad (4A)$$

$$C = 1.38 \times 10^{-15} \times (6.58 \times 10^{20} - 1.41 \times \sqrt{2.16 \times 10^{41} - 1.63 \times 10^{36} \cdot V_c}) \quad (5A)$$

Previous equations trace the evolution of forces in the joint as function of column shear, V_c , hence it is possible to evaluate the relevant $V_{c,i}$ triggering each considered failure mode. In particular, looking at the joint failure, column shear corresponding to the yielding failure of bars in tension into the beam or column, at the upper or lower side, can be evaluated by equating F_4 to minimum yielding force of beam reinforcement and F_3 to minimum yielding force of column reinforcement, respectively.

Such yielding forces of bars have to be calculated in advance. Since the reinforcement is symmetric, the minimum yielding force is simply evaluated by accounting for 5D16 ($A_{sb} = 1004.8 \text{ mm}^2$) in the beam and 4D19 ($A_{sc} = 1133.54 \text{ mm}^2$) in the column, so that yielding forces are:

$$F_{max,4} = A_s^{beam} \cdot f_y = 1004.8 \times 470 = 472,256 \text{ N} \quad (6A)$$

$$F_{max,3} = A_s^{column} \cdot f_y = 1133.54 \times 450 = 510,093 \text{ N} \quad (7A)$$

Hence the column shear corresponding to the failure due to the yielding of bars in beam, V_{c5} is equal to 121.73 kN and the column shear corresponding to the failure due to the yielding of bars in column, V_{c6} is equal to 128.33 kN, as it can be found in Table 5.

To evaluate the column shear leading to the failure due to reinforcement debonding, the bond capacity should be calculated. The bond capacity can be calculated as F_{bond} :

$$F_4 + S_1 = F_{bond} = n \cdot \pi \cdot \Phi \cdot L_{eb} \cdot \tau \quad (8A)$$

where n is the number of longitudinal bars, Φ is bar diameter, L_{eb} is the effective bond length and τ is the uniform bond stress capacity. Three conditions of bond have been considered. The case of maximum, medium and minimum bond capacities, namely $\tau_{max} = 13.23 \text{ MPa}$, $\tau_{med} = 6.61 \text{ MPa}$ and $\tau_{min} = 1.59 \text{ MPa}$, calculated according model Code 1990 [20]. Hence $F_{bondmax}$, $F_{bondmed}$, $F_{bondmin}$ are evaluated substituting the values of τ_{max} , τ_{med} and τ_{min} into the Equation (8A):

$$F_{bondmax} = 5\pi \times 16 \times 230 \times 13.23 = 764.31 \text{ kN} \quad (8Aa)$$

$$F_{bondmed} = 5\pi \times 16 \times 230 \times 6.61 = 382.15 \text{ kN} \quad (8Ab)$$

$$F_{bondmin} = 5\pi \times 16 \times 230 \times 1.59 = 91.72 \text{ kN} \quad (8Ac)$$

To evaluate bond demand $F_4 + S_1$ as a function of column shear V_c , the bar force in compression, S_1 , is extracted from the global compression force F_1 , as previously described. The whole section is assumed in the elastic range, hence it is possible to assess the neutral axis, c , by considering the static moment of the cracked section equal to zero (see Equation (11)). Compression force S_1 is evaluated according to Equation (12) as:

$$S_1 = 2.92 \times 10^{-25} \times (7.13 \times 10^{29} - 1.65 \times 10^9 \times \sqrt{2.16 \times 10^{41} - 1.63 \times 10^{36} \cdot V_c} + 5.97 \times 10^{23} \cdot V_c) \quad (9A)$$

where neutral axis, c , is equal to 47 mm. In this way, equating the bond demand to the bond capacity previously evaluated in the three bond conditions, it is possible to evaluate the column shears V_{c8} , V_{c9} and V_{c10} , respectively, as reported in Table 5 for the relevant simulation case.

Similarly V_{c11} corresponding to joint failure due to crushing of concrete strut is evaluated by equating C to $C_{\max} = 1,188$ kN, in this case (see Equation (9)).

It is now possible to evaluate failure modes due to bending and shear failures of beam and column. According to technical theory of flexure and shear capacity at ultimate state of RC beams and columns (e.g., in this case according to Italian practice [19]), the relevant values can be expressed as functions of the column shear (see Equations (6)–(8)). In the present case, relevant capacities are: beam flexural, $M_b = 142.50$ kNm, column flexural, $M_c = 90.19$ kNm, beam shear, $V_b = 423.23$ kN and column shear, $V_c = 328.58$ kN, directly equal to V_{c4} . These values yield to column shears V_{c1} to V_{c4} , respectively (Table 5). Due to changes of sign of fibers in tension and compression, the capacities are those minimum, hence evaluated accounting for the minimum reinforcement (in this case reinforcement is symmetric).

To identify the actual failure mode, the lowest column shear identifies the failure, and in this case (in good bond conditions) it is V_{c5} , hence a joint failure mode with yielding of bars in tension in the beam ($V_c = 121.5$ kN as reported in Table 6, slightly underestimating the experimental capacity, that is 130 kN, with the same reported joint failure mode).

As a concluding remark, to design a retrofit intervention, failure mode should be moved to beam flexural failure, hence joint should be improved to avoid a joint failure for a V_c smaller than $V_{c1} = 171.3$ kN (see Table 5). In any cases, having a clear summary of the column shears activating different failure modes for a beam column joint, it is possible to design a proper and effective retrofit intervention according to capacity design approach.

References

1. Manfredi, G.; Verderame, G.M.; Lignola, G.P. A F.E.M. Model for the Evaluation of the Seismic Behavior of Internal Joints in Reinforced Concrete Frames. In Proceedings of the 14th World Conference on Earthquake Engineering, Beijing, China, 12–17 October 2008.
2. Lignola, G.P.; Verderame, G.M.; Manfredi, G. Effect of Bond on Seismic Performance of Internal Joints in Reinforced Concrete Frames. In Proceedings of the 14th European Conference on Earthquake Engineering, Ohrid, Republic of Macedonia, 30 August–3 September 2010.
3. Masi, A.; Santarsiero, G.; Lignola, G.P.; Verderame, G.M. Study of the seismic behaviour of external RC beam–column joints through experimental tests and numerical simulations. *Eng. Struct.* **2013**, *52*, 207–219. [[CrossRef](#)]
4. Alcocer, S.M.; Jirsa, J.O. Strength of reinforced concrete frame connections rehabilitated by jacketing. *ACI Struct. J.* **1993**, *90*, 249–261.
5. Ghobarah, A.; Aziz, T.S.; Biddah, A. Rehabilitation of reinforced concrete frame connections using corrugated steel jacketing. *ACI Struct. J.* **1997**, *94*, 282–294.
6. Tsonos, A.G. Lateral load response of strengthened reinforced concrete beam-column joints. *ACI Struct. J.* **1999**, *96*, 46–56.
7. Hakuto, S.; Park, R.; Tanaka, H. Seismic load tests on interior and exterior beam-column joints with substandard reinforcing details. *ACI Struct. J.* **2000**, *97*, 11–25.
8. Gergely, I.; Pantelides, C.P.; Reaveley, L.D. Shear Strengthening of Bridge Joints with Carbon Fiber Composites. In Proceedings of Sixth US National Conference on Earthquake Engineering, Seattle, WA, USA, 31 May–4 June 2008.

9. Pantelides, C.; Clyde, C.; Dreaveley, L. Rehabilitation of R/C building Joints with FRP Composites. In Proceedings of the 12th World Conference on Earthquake Engineering, Auckland, New Zealand, 30 January–4 February 2000.
10. Gergely, J.; Pantelides, C.P.; Reaveley, L.D. Shear strengthening of RCT-joints using CFRP composites. *J. Compos. Construct.* **2000**, *4*, 56–64. [[CrossRef](#)]
11. Granata, P.J.; Parvin, A. An experimental study on kevlar strengthening of beam-column connections. *J. Compos. Struct.* **2001**, *53*, 163–171. [[CrossRef](#)]
12. Ghobarah, A.; Said, A. Seismic rehabilitation of beam-column joints using FRP laminates. *J. Earthquake Eng.* **2001**, *5*, 113–129. [[CrossRef](#)]
13. Pantelides, C.P.; Okahashi, Y.; Reaveley, L.D. Seismic rehabilitation of reinforced concrete frame interior beam–column joints with FRP. *J. Compos. Constr.* **2008**, *12*, 435–445. [[CrossRef](#)]
14. Paulay, T.; Park, R.; Priestley, M.J.N. Reinforced concrete beam-column joints under seismic actions. *J. ACI* **1978**, *75*, 585–593.
15. Uma, S.R.; Jain, S.K. Seismic design of beam–column joints on RC moment resisting frames—Review of codes. *Struct. Eng. Mech. Int. J.* **2006**, *23*, 579–597. [[CrossRef](#)]
16. Shiohara, H. New model for shear failure of RC interior beam–column connections. *J. Struct. Eng.* **2001**, *127*, 152–160. [[CrossRef](#)]
17. Lowes, L.N.; Altoontash, A. Modeling reinforced-concrete beam–column joints subjected to cyclic loading. *J. Struct. Eng.* **2003**, *129*, 1686–1697. [[CrossRef](#)]
18. Kim, J. Joint Shear Behavior of Reinforced Concrete Beam-column Connections Subjected to Seismic Lateral Loading. Ph.D. Thesis, University of Illinois, Urbana-Champaign, MI, USA, 2007.
19. Cosenza, E.; Manfredi, G.; Pecce, M. *Strutture in Cemento Armato: Basi Della Progettazione*; HOEPLI: Milan, Italy, 2008. (In Italian)
20. CEB-FIP Model Code 90 “Design Code”. Thomas Telford Services Ltd.: London, UK, 1990.
21. Advisory Committee on Technical Recommendations for Construction. *Guide for the Design and Construction of Externally Bonded FRP Systems for Strengthening Existing Structures*; National Research Council: Roma, Italy, 2013.
22. Hakuto, S.; Park, R.; Tanaka, H. Effect of deterioration of bond of beam bars passing through interior beam-column joints on flexural strength and ductility. *ACI Struct. J.* **1999**, *96*, 858–864.
23. Prota, A.; Nanni, A.; Manfredi, G.; Cosenza, E. Selective upgrade of underdesigned reinforced concrete beam–column joints using carbon fiber-reinforced polymers. *ACI Struct. J.* **2004**, *101*, 699–707.
24. Zaid, S.; Shiohara, H.; Otani, S. Test of a Joint Reinforcing Detail Improving Joint Capacity of R/C Interior Beam–Column Joint. In Proceedings of the 1st Japan-Korea Joint Seminar on Earthquake Engineering for Building Structures, Seoul National University, Seoul, South Korea, 29 October 1999.